



Subcell Debye behavior analysis of order–disorder effects in triple-junction InGaP-based photovoltaic solar cells



Jui-Ju Hsiao^a, Hung-Ing Chen^a, Yi-Jen Huang^a, Jen-Cheng Wang^a, Bing-Yuh Lu^b,
Ya-Fen Wu^c, Tzer-En Nee^{a,*}

^a Graduate Institute of Electro-Optical Engineering and Department of Electronic Engineering, Chang Gung University, 259 Wen-Hwa 1st Road, Kwei-Shan, Tao-Yuan, Taiwan ROC

^b Department of Electronic Engineering, Tunghnan University, No.152, Sec. 3, Beishen Road, Shenkeng District, New Taipei City, Taiwan ROC

^c Department of Electronic Engineering, Ming Chi University of Technology, 84 Gungjuan Road, Taishan District, New Taipei City, Taiwan ROC

ARTICLE INFO

Article history:

Received 4 February 2015

Received in revised form

3 August 2015

Accepted 6 August 2015

Available online 21 August 2015

Keywords:

Debye temperature

Disordered

Ordered

Photoluminescence

Photon–phonon coupling coefficient

Photovoltaic solar cells

ABSTRACT

Analysis was made of the Subcell Debye behavior of the order–disorder effects in triple-junction InGaP-based photovoltaic solar cells fabricated by a metal organic vapor phase epitaxy (MOVPE) system with careful adjustment of the growth conditions. The order–disorder configurations of the InGaP subcells were investigated after post-annealing treatment at various temperatures in a nitrogen atmosphere. Temperature-dependent photoluminescence (PL) measurements over a broad temperature range provided insight into the roles of the thermophysical phenomena connected with the ordering and disordering in the InGaP alloys. The thermally-related spectroscopic observations associated with the ordering effects on the photon–phonon interactions were confirmed by the McCumber–Sturge theory. The variations of both the full width at half-maximum (FWHM) and shift in the peak of PL with temperature were analyzed. According to the width-related PL observations the effective photon–phonon coupling coefficient and the Debye temperature were 0.53 meV and 424 K, respectively; according to shift-related PL observations of the as-grown sample they were 0.3247 eV and 430 K, respectively, for the width-related PL observation they were 0.29 meV and 421 K; and from the shift-related PL observations for the as-grown ordered samples they were 0.3142 eV and 425 K, respectively, implying that the spontaneously disordered InGaP heterostructures met the demand for improvement of photovoltaic devices. Both the effective photon–phonon coupling coefficient and the Debye temperatures were characterized as functions of the annealing temperature. The Debye temperatures obtained for the disordered and ordered top subcells were consistent with the universal Gruneisen–Bloch relation.

© 2015 Elsevier B.V. All rights reserved.

1. Introduction

Although Adachi et al. did examine the characteristics of a zincblende binary compound by using the Debye model [1], there have been few studies of the lattice thermal properties of ternary compounds. Theoretically, multi-junction photovoltaic (PV) devices are expected to have the highest limit of efficiency conversion compared to other heterostructure designed solar cells [2]. The conversion efficiency of a solar cell is intrinsically a function of its band heterostructure and the device performance of multi-junction solar cells is strongly governed by the individual characteristics of the respective

subcells. The assessment of the subcell features thus plays an essential role in further optimization of multi-junction solar cell heterostructures and devices. Accurate knowledge of the subcell properties is of course not only important for device engineering, but also to obtain a clear understanding from physical perspectives. The performance of solar cells is inherently associated with the photon–electron interaction occurring in well-designed heterostructures. Different subcell combinations have been proposed to improve the external quantum efficiency of multi-junction photovoltaic devices by alleviating the problems of current mismatching and luminescence coupling [3,4]. Many characterization techniques for individual subcells have also been developed based on the optoelectronic reciprocity relation [5].

It is widely believed that using a top subcell material with higher bandgap is critically important in the design of the most efficient multi-junction photovoltaic solar cells. The lattice matc-

Abbreviations: FWHM, Full width at half-maximum; MOVPE, Metal organic vapor phase epitaxy; PL, Photoluminescence; PV, Photovoltaic.

* Corresponding author. Tel.: +886 3 2118800x5791; fax: +886 3 2118507.

E-mail address: neete@mail.cgu.edu.tw (T.-E. Nee).

hing of the InGaP top subcell to GaAs to increase the transparency to incident light is helpful for the design of a better triple-junction InGaP-based solar cell. As a matter of fact, the promise of multi-junction InGaP-based metamorphic cells that provide high conversion efficiency has been realized using top subcell structures with indium mole fractions of about 50% [6]. Furthermore, thinning of the top subcell is considered to result in significant increases in amount of the light passing through to the middle subcell for current matching. These effects act to increase the light absorption of the middle cell and the voltage of the top subcell by a group-III sublattice disordered top subcell, allow the spontaneously disordered InGaP heterostructures to meet the demand for improvement in the external quantum efficiency of PV devices [7]. The photon–phonon coupling processes occurring in the top subcell can be understood using the theory developed by McCumber and Sturge which is based on the so-called zero-phonon assumption. This is considered a feasible approach for evaluating the photoresponse characteristics of ordered and disordered samples [8,9]. On the other hand, it is also known that the wide range of operating temperature of monolithic multijunction solar cells, from below-zero to over 100 °C, can lead to spatial fluctuations of the sublattices. Problem arising from thermal equilibrium is inherent to the so-called annealing effects on the ordered and disordered subcells, resulting in a shift and broadening of the emission spectra [10,11]. Accordingly, a good-understanding of how ordered and disordered subcells behave in response to changes in temperature is necessary for optimizing device performance at any operating temperature [12–14]. Since not only thermal luminescent broadening but also a thermal luminescent shift can be produced by the simultaneous interaction of the incident radiation and the lattice vibration, it is instructive to describe the corresponding energy changes associated with the InGaP alloy configurations in terms of the characteristic Debye temperatures [15].

In this work, triple-junction InGaP-based solar cells composed of ordered and disordered InGaP top subcells were produced by metal organic vapor phase epitaxy (MOVPE) with careful adjustment of the growth conditions. Temperature-dependent photoluminescence (PL) measurements made over a broad temperature range provide insight into the roles of the thermophysical phenomena connected with the ordering and disordering of InGaP alloys used in the top subcells. The samples investigated were treated by post-annealing at various temperatures in a nitrogen atmosphere in order to modulate the order–disorder configurations of the InGaP alloys. From the viewpoint of quantum mechanics, the high-temperature treatment processes correspondingly modified both the vibrational eigenfrequencies and eigenvectors of normal modes, giving rise to interesting coupling problems. However, due to the lack of the translational invariance of the disordered lattices, it is rarely possible, even with the sophisticated analytical techniques that have been developed, to deal with the luminescent properties of thermal excitation existing in the ordered/disordered solids in a satisfactory manner. One most proper way to approach the thermal-induced vibrational mode properties of ordered/disordered solids was the well-developed phonon gas model [16]. The temperature-dependent radiative characteristics, including both shift and broadening, responsible to the energy distribution changes were accounted for by the creation or annihilation of phonons [17].

The thermal-related spectroscopic observations associated with the ordering effects on the photon–phonon interactions were assessed based on the McCumber–Sturge theory. The effective photon–phonon coupling coefficients and the Debye temperatures were characterized as functions of the annealing temperature. The Debye temperatures obtained for the ordered and disordered top subcells were consistently corroborated by the universal Gruneisen–Bloch

relation. In our study, the experimental results provide the basis for a simple discussion about InGaP top Subcell Debye behavior analysis of order–disorder effects.

2. Experimental methods

All devices were grown using the standard MOVPE process. The subcells (InGaP, GaAs and Ge junctions) of the triple-junction solar cell were grown on a p-type Ge substrate. The InGaP subcell was connected to the GaAs subcell by a p-AlGaAs/n-InGaP tunnel junction. The GaAs subcell was connected to the Ge subcell by a p-GaAs/n-GaAs tunnel junction. The $\text{In}_{0.49}\text{Ga}_{0.51}\text{P}$ top, GaAs middle, and Ge bottom subcells were all lattice-matched. There were two different types of samples used in this study. The high doped disordered InGaP top subcell grown at 730 °C with larger band gaps, and the low doped ordered InGaP top subcell grown at 675 °C with a smaller band gap.

The samples were investigated after undergoing post-annealing treatment at various temperatures ranging from 100 °C to 400 °C for 30 min in a nitrogen atmosphere. For the temperature-dependent PL measurements, the samples were mounted in a closed-cycle He cryostat and excited with the 633 nm line from an He–Ne laser. These measurements were taken in the temperature range of 20–300 K, every 20 K. Since the measurement temperature was notably lower than the annealing temperature, it allows the presence of the change in orientational and positional disorder, i.e., so-called static disorder, to be ignored as temperature rising up to 300 K. The luminescence signal was dispersed through a 0.5-meter monochromator and later detected by a Si photodiode, employing the standard lock-in amplification technique.

Based on the zero-phonon model, the McCumber–Sturge theory can be used to describe the photon–phonon coupling in conjunction with the spectroscopic experiments. The FWHM variation and peak shift with temperature were expressed by

$$\Delta\omega(T) = \alpha \left(\frac{T}{\theta_D} \right)^4 \int_0^{\frac{\theta_D}{T}} \frac{x^3 e^x}{(e^x - 1)^2} dx \quad (1)$$

and

$$\Delta\Gamma(T) = \alpha \left(\frac{T}{\theta_D} \right)^7 \int_0^{\frac{\theta_D}{T}} \frac{x^6 e^x}{(e^x - 1)^2} dx, \quad (2)$$

respectively, $\Delta\omega(T)$ indicates the peak shift with temperature, i.e., the difference between the peak energies at temperature T and at 20 K, where $\Delta\Gamma(T)$ indicates the temperature-dependent FWHM variation, i.e., the difference between the linewidths at temperature T and at 20 K, α might be assigned to the photon–phonon coupling constant, and θ_D is the characteristic Debye temperature. Taking natural logarithms of both sides of Eqs. (1) and (2) and rearranging terms, we obtain the following expression:

$$\ln[\Delta\xi(T)] - \ln \left[\int_0^{\frac{\theta_D}{T}} \frac{x^{a-1} e^x}{(e^x - 1)^2} dx \right] = a \ln \left(\frac{T}{\theta_D} \right) + \ln \alpha. \quad (3)$$

where $\Delta\xi(T)$ indicates the temperature-dependent spectral variations, as mentioned above. To proceed further with this non-linear analysis, it is convenient to obtain the power law of the temperatures through a log–log plot. Assuming a quasi-constant value for the photon–phonon coupling constant with respect to the ratio of the measured temperature and Debye temperature, we obtain a straight line as defined by Eq. (2) with a slope of a on the log–log scale. The value of the power law index, i.e., a , was dependent on the spectral behavior concerned. It has been found that the peak shift and the linewidth variation varied as T^4 and T^7

at temperatures lower than Debye temperature, i.e., the corresponding indices were 4 and 7, respectively, while those varied as T and T^2 at temperatures higher than Debye temperature, i.e., the corresponding indices were 1 and 2, respectively [18,19]. The corresponding extrapolated intercepts were effectively the photon-phonon coupling coefficients where the interactions of the incident photons and the lattice vibrations were described in terms of two different types of spectral examinations, thermal-induced peak shift and width spreading.

3. Results and discussion

The dependence of the ordering–disordering effects on the annealing temperature can be evaluated and, characterized by examining the Debye behavior of the InGaP subcell under optical excitation. A Debye temperature is a single parameter that contains information about vibration frequencies related to the lattice vibration of material systems [20]. Fig. 1 shows the low temperature PL spectra of disordered and ordered top subcells. The spectra clearly reveal an emission peak located at around 1.87 eV. Shu et al. study has obtained the photoluminescence (PL) spectra of the three junction InGaP/InGaAs/Ge solar cell using three different excitation lasers. The spectra clearly reveal an InGaP signal located at around 1.9 eV and a GaAs signal located at around 1.5 eV, which originated from the top and middle subcells, respectively [21]. These two samples have a 10 meV difference in their peak energy that coincides with that discussed in Romero et al. The group found that the CL spectra also show indications of a radiation induced order–disorder transition in the InGaP. The proton irradiation causes an energy shift of 10 meV (at $T=70$ K) in the InGaP luminescence peak [22]. The photon energy and linewidth of the PL spectra for the ordered and disordered samples as a function of temperature were extracted by deconvoluting the luminescence spectra using a Gaussian fit. The spectral peak and the FWHM for the as-grown disordered sample at 20 K were 1.87 eV and 12.14 meV, respectively; those same values were 1.86 eV and 15.11 meV, respectively for the as-grown ordered sample at 20 K (not shown here). Compared to the ordered InGaP alloy, the disordered InGaP alloy exhibited a higher transition energy, as reported elsewhere [23–25]. This is due to the electron–hole recombination which occurs in an ordered active layer with a narrower band gap. Furthermore, the experimental observations presented in Fig. 2 show the variation in the photon energy and the FWHM in response to the changes of temperature in the samples annealed at different temperatures. There is a redshift in the emission peaks for the ordered and disordered subcells with

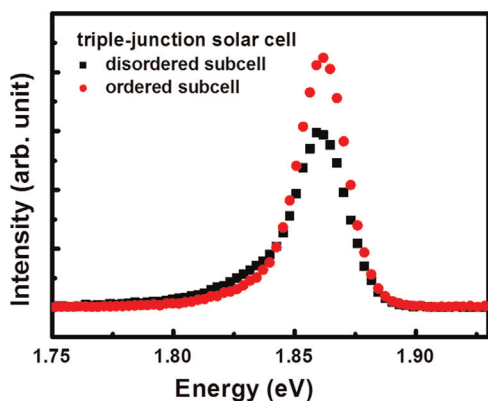


Fig. 1. Photoluminescence (PL) spectra of the three-junction solar cell obtained using an He–Ne laser at 20 K. The spectra clearly reveal an InGaP signal located at around 1.86 eV.

increased measuring temperatures, indicating temperature-induced bandgap shrinkage of the ternary InGaP structure [26–28]. Due to the random configuration of the carriers photo-generated in the disordered and ordered subcells, the radiative energy may be defined as the free energy from electron–hole pairs created, with no phonons being involved. This provides a clear picture of the observations of the thermal dependent shifts modulated by the annealing temperature. The free energy $\Delta E(T)$ can be decomposed into the transition enthalpy $\Delta H(T)$ and transition entropy $\Delta S(T)$ as follows: $\Delta E(T) = \Delta H(T) - T\Delta S(T)$ [29–34]. Consequently, the entropy revealing the amount of ordering and disordering in a thermodynamic system at a given measuring temperature can be determined from the slope as indicated by the dashed lines in Fig. 2(a) and (b). The values of Debye temperature, spectral linewidth, peak energy, and statistical entropy deduced at 20 K for the two samples treated with different annealing temperatures are listed in Table 1. The entropy statistically describes spontaneous fluctuations in the irreversible generation–recombination processes in the subcells which decrease with increasing annealing temperature (within the limits of experimental accuracy), suggesting the occurrence of a micro-recrystallization process at a high annealing temperature. The width of the zero-phonon line was usually only a few tens of milli-electron volts (meV). The temperature-dependence of the FWHM variation over a broad temperature range has the potential for the fabrication of a sensitive probe, which could be used to study the thermo-photo-electrical phenomena connected with the ordering and disordering of InGaP alloys, as shown in Fig. 2(c) and (d). The change in FWHM with temperature is larger for disordered samples than ordered samples after post-annealing. There was a notable broadening in the observed spectral linewidths in both types of subcell which was associated with the photocarrier thermalization process arising from the interaction between the incident light and vibrating lattice [32]. This was phenomenologically consistent with the diminishing entropy, as presented in Table 1. The post-annealing temperature effectively depressed the thermal luminescent broadening. The disordered top subcell transformed to an ordered lattice structure when the annealing temperature was higher than 200 °C. The change in entropy was low when the temperature was less than 200 °C, and gradually decreased with increasing annealing temperature. Moreover, we found a significantly larger change in the FWHM of the disordered samples than that for the ordered ones, which was related to the enhancement of the photon–phonon coupling in the disordered configuration.

To better understand how the annealing process influences the structural configuration which inherently govern the optical properties, we take the unique approach of using the McCumber–Sturge theory [33,34] to assess these thermal-related spectroscopic observations associated with structural ordering effects on photon–phonon interactions from the viewpoint of particles. Excluding the exceptional deviations, the power-law indices for the shift-related and width-related features were essentially equal to 7 and 4, respectively, which is in good agreement with the afore-mentioned power law at temperatures lower than Debye temperature; see the dashed lines in Fig. 3. These lines were obtained from the slopes of the plots of $\ln[\Delta\xi(T)] - \ln[\int x^{a-1}e^x(e^x - 1)^{-2}dx]$ versus $\ln(T/\theta_D)$ for both samples, as has been mentioned above. The departure of the slopes from 7 and 4 in the low temperature regime is expected to reflect the presence of the characteristic Debye temperature as indicated in Eq. (2) and is temperature-sensitive. As far as the extrapolation intercepts of the lines in Fig. 3 are concerned, it was numerically found that the shift-related photon–phonon coupling coefficients extracted from the observations in Fig. 2(a) and (b) for the as-grown disordered and ordered samples were 0.3247 and

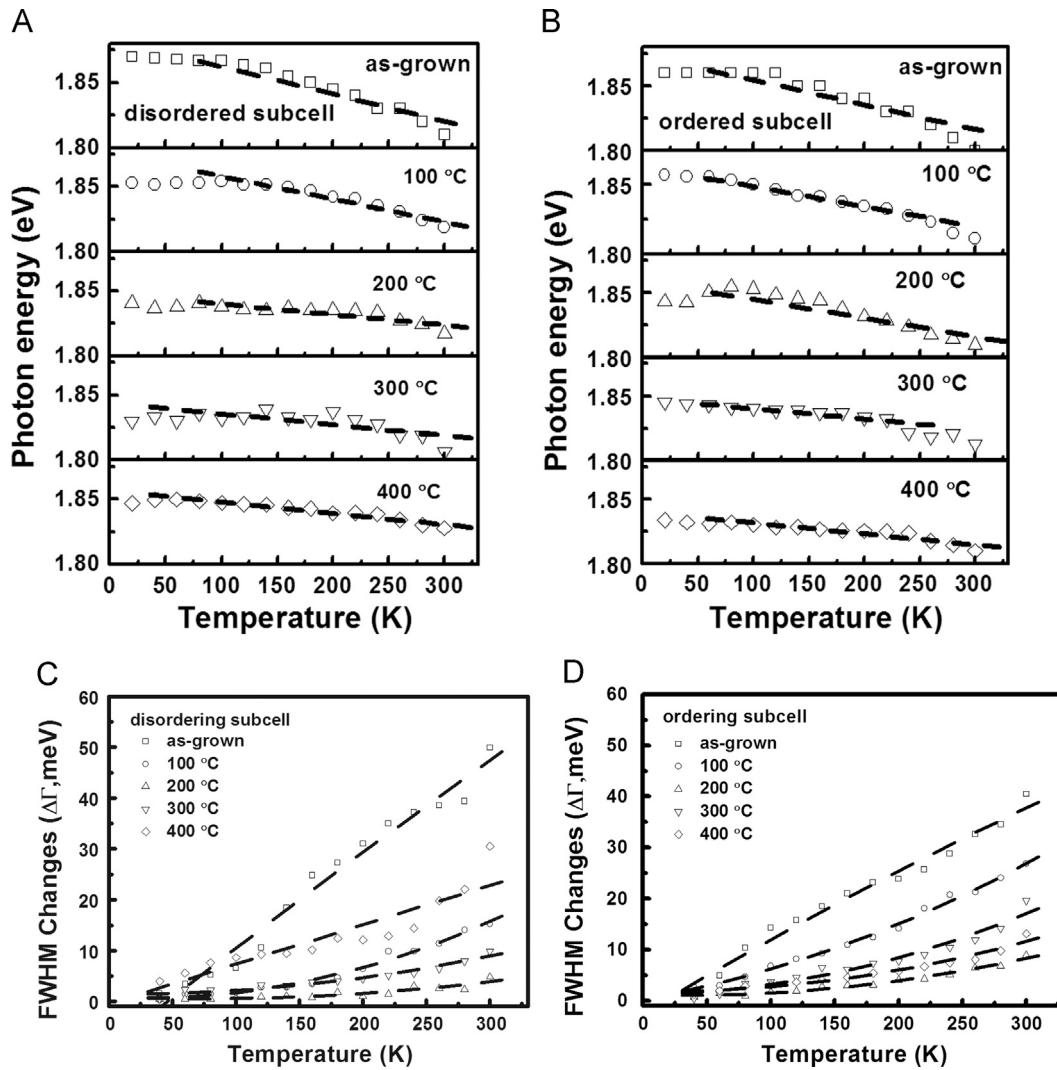


Fig. 2. (a, b) Photon energy and (c, d) FWHM variation in response to changes in temperature for both the disordered and ordered samples annealed at different temperatures. The temperature-dependence of the FWHM over a broad temperature range has potential for the development of a sensitive probe with which to study thermo-photoelectrical phenomena connected with the ordering and disordering of InGaP alloys.

Table 1

The values of peak energy, spectral linewidth, Debye temperature, and entropy at 20 K for the two samples treated with different annealing temperatures.

Annealing temperature (°C)	ω_0 (eV)		Γ_0 (meV)		θ_D (K)				Entropy (10^{-4} meV/K)	
	Disordered	Ordered	Disordered	Ordered	Shift		FWHM		Disordered	Ordered
					Disordered	Ordered	Disordered	Ordered		
As-grown	1.846	1.834	12.14	15.11	430	425	425	421	2.1	1.9
100	1.83	1.845	42.9	30.1	415	413	408	407	1.7	1.4
200	1.84	1.843	14.9	10.97	408	400	401	400	0.8	1.4
300	1.852	1.856	57.25	40.51	410	405	403	402	0.84	0.8
400	1.869	1.86	50	48.29	412	407	410	404	0.87	0.84

0.3142 eV, respectively, while the width-related values of those extracted from the observations in Fig. 2(c) and (d) for those samples were 0.53 and 0.29 meV, respectively. There is minor change due to temperature-dependence of the photon–phonon coupling constants in this system. Thus, it is assumed in this study that the photon–phonon coupling constant is a quasi-constant value. The temperature-dependence of the photon–phonon coupling constant was also analyzed for other systems. (The results of which will be published elsewhere.) Comparison shows that the photon–phonon coupling coefficients of the ordered sample were lower than for the

disordered sample, indicating the possibility of improving the multi-junction solar cell performance by adopting an ordered top subcell. It is well-known that the photon–phonon interaction can be different for phonons involved in line broadening mechanisms as regards to those involved in line-shifting mechanisms, leading to the discrepancy in the coupling coefficients deduced from these two different analyzes [35]. Accordingly, since thermally-induced broadening is considerably more sensitive than thermally-induced shifting with increasing temperature above 100 K, the linewidth-related photon–phonon coupling coefficient was usually larger than

the shift-related photon–phonon coupling coefficients for both of the samples.

In order to grasp the essence of the annealing effect on the optical properties of the top subcells, the variations of both peak shifts and FWHM changes of PL with measurement temperature at the applied annealing temperature were analyzed (procedures were similar to those used for Fig. 3). The photon–phonon coupling coefficients as a function of the annealing temperature for both the disordered and ordered samples are plotted in Fig. 4. The as-grown samples showed a decrease in the shift-related and linewidth-related coupling coefficients for both samples with annealing temperatures up to 200 °C, but then an increased with annealing temperatures up to 400 °C. This arose from the thermal renormalization of statistical entropy at the given annealing temperatures, as discussed above. According to the modified Williams–Mathews formulism, the effect of randomness gives rise to broadened energy bands in an ordered lattice system [36]. In order to there are more localized states existing in the bandgap of a disordered lattice system. The number of localized states outside the band increases with an increase in the disordering of the lattices. The state disordering is related to the structural disordering. The FWHM results were inconsistent with state disordering, we infer that the sample is in a state of structural disorder. The overlapped states existing in the disordered lattice are a combination of localized and delocalized states. Consequently, compared with the ordered lattices, both the density of states and the average crystal momentum of the disordered materials can be extended to much wider energy distributions in the characteristic momentum space. With respect to the symmetry principle, because of the presence of the aperiodic fluctuation processes in the top subcells, the translational invariance of the periodic

lattices is broken down. Due to this, the selection rule of optical transitions is intrinsically relaxed at the long-wavelength approximation, and well-organized disordering in the top cell is facilitates by the enhancement of the photon–phonon coupling efficiency of multi-junction solar hetero devices.

It is interesting to describe a heterostructure in equilibrium using a functional relationship between the thermodynamic variable defined in a unified picture. These two coupling coefficients circumscribed in different domains can be qualitatively understood in terms of the characteristic Debye temperature responding to the random configurations in the subcells over the annealing temperature range. According to the McCumber–Sturge formulation, the Debye temperatures extracted from the observations in Fig. 2 can be characterized as a function of the applied annealing temperature, as plotted in Fig. 5. Consequently, it can be clearly seen that the dependence of the Debye temperature on the annealing-temperature is similar to the coupling constant features presented in Fig. 4. Using the Debye model we can approximately fit the photon–phonon coupling, but the Debye model is not consistent at low temperature, as seen in Fig. 3. Prior to a discussion of the relevance between the characteristic temperature and the photon–phonon interaction, it is instructive to numerically estimate the Debye temperature based on the lattice dynamics developed in the solid thermodynamics for comparison. Although the elastic constants of most of the III–V compound semiconductors are well-known, there is less information available about the influence of detailed ordering of the elastic parameters over a wide range of temperatures. From knowledge of the elastic coefficients of InGaP lattice matched to GaAs empirically obtained using Vegard’s law, we find that the sound velocity is numerically equal to 5.17×10^5 cm/s. The Debye temperature θ_D can be

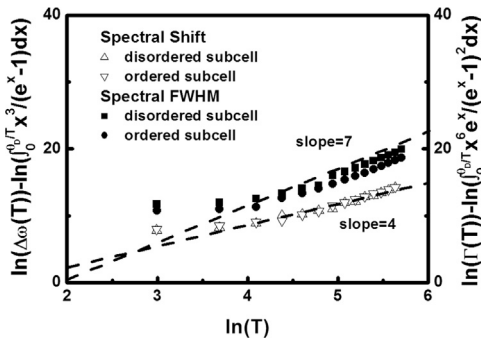


Fig. 3. The McCumber–Sturge theory is used to assess the thermal-related spectroscopic observations associated with the structure and ordering–disordering effects on photon–phonon interactions.

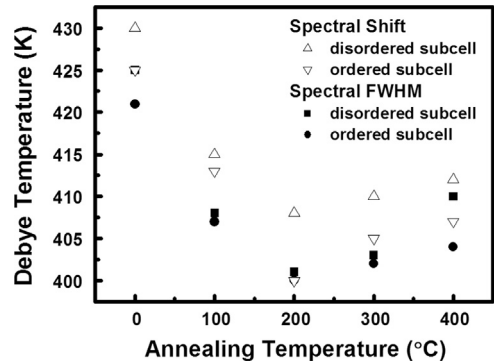


Fig. 5. The annealing-temperature dependence showing the Debye temperature for disordered and ordered samples.

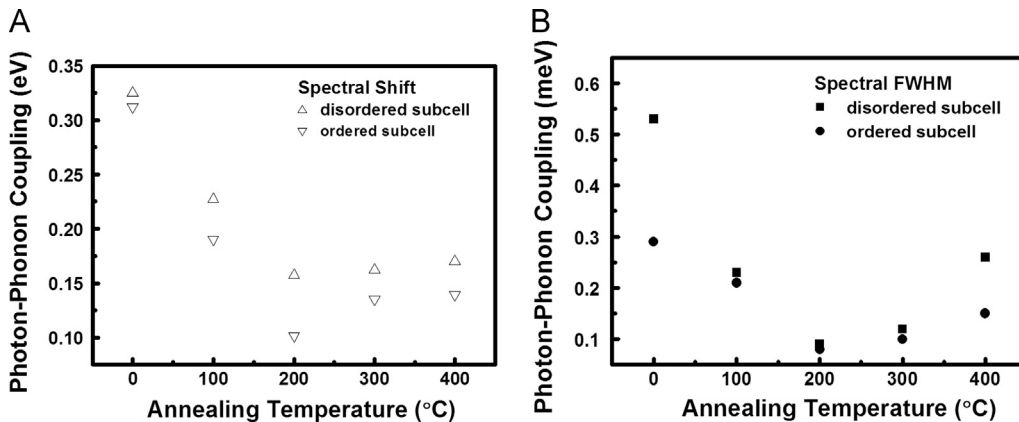


Fig. 4. The photon–phonon coupling coefficients as a function of the annealing temperature for the disordered and ordered samples.

approximately determined to be 450 K by $\theta_D = \frac{h}{k_B} \left[\frac{3q N \rho}{4\pi M} \right]^{\frac{1}{3}} v_m$, where h/k_B has the usual meaning used in quantum mechanics, q is the number of atoms in the molecule, N is the Avogadro's number, ρ is the density, M is the molecular weight of the solid, and v_m is the sound velocity. As can be recognized from the argument above, the Debye temperature is associated with the lattice vibrations governed by the thermally-induced change in the structural entropy to the respective subcells, resulting in the photon–phonon couplings examined in terms of the line-shifting and the line-broadening characteristics. Based on the solid statistical descriptions, the allowed volume of the Debye sphere was heavily perturbed by the heat treatment temperature, leading to the Debye temperature of the disordered lattice being larger than that of the ordered one. This certainly had a substantial effect on the spectroscopic observations. As presented in Figs. 2 and 5, the proper post-annealing procedure not only diminishes the lattice aperiodicity but also reduces the Debye temperature, while the improper high temperature might lead both to randomizing periodicity and to increasing the Debye temperature.

4. Conclusions

The subcell Debye behavior of the order–disorder effects in triple-junction InGaP-based photovoltaic solar cells produced by a MOVPE system after careful adjustment of the growth conditions was analyzed. The order–disorder configurations of the InGaP subcells were investigated after post-annealing treatment at various temperatures in a nitrogen atmosphere. Temperature-dependent PL measurements over a broad temperature range provided insight into the roles of the thermophysical phenomena connected with the ordering and disordering of InGaP alloys. These thermal-related spectroscopic observations associated with ordering effects on photon–phonon interactions were assessed by comparison with the McCumber–Sturge theory. Analysis of the variations in both the FWHM and peak shift of PL with temperature gave rise to an effective photon–phonon coupling coefficient and Debye temperatures for the as-grown disordered sample of 0.53 meV and 424 K, respectively, from width-related PL observations and 0.3247 eV and 421 K from shift-related PL observations those values were 0.29 meV and 430 K from width-related PL observations and 0.3142 eV and 425 K from shift-related PL observations for the as-grown ordered samples. It was also found that both the effective photon–phonon coupling coefficient and the Debye temperatures could be characterized as function of the annealing temperature. The obtained Debye temperatures of the disordered and ordered top subcells were consistent with the universal Gruneisen–Bloch relation. The assessment of the ordered and disordered InGaP subcell features is expected to play a crucial role in the further optimization of multi-junction solar cell heterostructures and devices.

Acknowledgments

The authors would like to acknowledge support from the staff of QUEST Laboratory (Quantum Electro-optical Science and Technology Laboratory), Graduate Institute of Electro-Optical Engineering and Department of Electronic Engineering, Chang Gung University, Taiwan. This study was financially supported by the Ministry of Science and Technology, ROC under Contract no. MOST 103-2112-M-182-001 and 104-2112-M-182-002.

References

- [1] S. Adachi, *J. Appl. Phys.* 58 (1985) R1.
- [2] R.R. King, D. Bhusari, D. Larrabee, X.Q. Liu, E. Rehder, K. Edmondson, H. Cotal, R.K. Jones, J.H. Ermer, C.M. Fetzer, D.C. Law, N.H. Karam, *Prog. Photovolt. Res. Appl.* 20 (2012) 801.
- [3] J.J. Li, S.H. Lim, C.R. Allen, D. Ding, Y.H. Zhang, *IEEE J. Photovolt.* 1 (2011) 225.
- [4] S.H. Lim, J.J. Li, E.H. Steenbergen, Y.H. Zhang, *Prog. Photovolt. Res. Appl.* 21 (2013) 344.
- [5] S. Roensch, R. Hoheisel, F. Dimroth, A.W. Bett, *Appl. Phys. Lett.* 98 (2011) 251113.
- [6] M.J. Yang, M. Yamaguchi, T. Takamoto, E. Ikeda, H. Kurita, M. Ohmori, *Sol. Energy Mater. Sol. Cells* 45 (1997) 331.
- [7] T. Suzuki, A. Gomyo, I. Hino, K. Kobayashi, S. Kawata, S. Iijima, *Jpn. J. Appl. Phys.* 27 (1988) L1549.
- [8] I.I. Abram, *Chem. Phys.* 25 (1977) 87.
- [9] G.J. Small, *Chem. Phys. Lett.* 15 (1972) 147.
- [10] J. Dekker, A. Tukiainen, N. Xiang, *J. Appl. Phys.* 86 (1999) 3709.
- [11] M. Guina, J. Dekker, A. Tukiainen, *J. Appl. Phys.* 89 (2001) 1151.
- [12] Y.C. Cheng, S. Chi, S.T. Chou, K.F. Huang, *Jpn. J. Appl. Phys.* 39 (2000) L968.
- [13] Y. Hamisch, R. Steffen, P. Rontgen, A. Forchel, *Jpn. J. Appl. Phys.* 32 (1993) L1492.
- [14] Y.C. Cheng, K. Tai, S.T. Chou, *Jpn. J. Appl. Phys.* 39 (2000) L819.
- [15] A. Joshi, M.O. Manasreh, E.A. Davis, B.D. Weaver, *Appl. Phys. Lett.* 89 (2006) 111907.
- [16] C. Kittel, *Quantum Theory of Solids*, second revised ed., Wiley, New York, 1987.
- [17] G.P. Srivastava, *The Physics of Phonons*, zeroth ed., CRC, London, 1990.
- [18] A. Kuznetsov, A. Laisaar, J. Kikas, *Opt. Mater.* 32 (2010) 1671.
- [19] G.F. Imbusch, W.M. Yen, A.L. Schawlow, D.E. McCumber, M.D. Sturge, *Phys. Rev.* 133 (1964) A1029.
- [20] G. Grimvall, *Thermophysical Properties of Materials*, first ed., North Holland, New York, 1999.
- [21] G.W. Shu, C.H. Tung, S.C. Tung, P.C. Su, J.L. Shen, M.D. Yang, C.H. Wu, W.C. Chou, C.H. Ko, *Jpn. J. Appl. Phys.* 50 (2011) 092302.
- [22] M.J. Romero, D. Araujo, R. Garcia, *Appl. Phys. Lett.* 74 (1999) 2684.
- [23] M.K. Lee, R.H. Horng, L.C. Haung, *J. Appl. Phys.* 72 (1992) 5420.
- [24] Y. Dong, R.M. Feenstra, M.P. Semtsiv, W.T. Masselink, *J. Appl. Phys.* 103 (2008) 073704.
- [25] Jr. R.P. Schneider, E.D. Jones, J.A. Lott, R.P. Bryan, *J. Appl. Phys.* 72 (1992) 5397.
- [26] K.L. Teo, J.S. Colton, P.Y. Yu, E.R. Weber, M.F. Li, W. Liu, K. Uchida, H. Tokunaga, N. Akutsu, K. Matsumoto, *Appl. Phys. Lett.* 73 (1998) 1697.
- [27] N.J. Quitoriano, E.A. Fitzgerald, *J. Appl. Phys.* 102 (2007) 033511.
- [28] X.B. Zhang, J.H. Ryoo, R.D. Dupuis, G. Walter Jr., N. Holonyak, *Appl. Phys. Lett.* 87 (2005) 201110.
- [29] C.M. Penchina, J.S. Moore, *Phys. Rev. B* 9 (1974) 5217.
- [30] T. Pullerits, K.J. Visscher, S. Hess, V. Sundstrom, A. Freiberg, K. Timpmann, R. V. Grondelle, *Biophys. J.* 66 (1994) 236.
- [31] D.C. Wong, C.M. Penchina, *Phys. Rev. B* 12 (1975) 5840.
- [32] J.T. Darrow, X.C. Zhang, D.H. Auston, *Appl. Phys. Lett.* 58 (1991) 25.
- [33] S. Smith, A. Mascarenhas, S.P. Ahrenkiel, M.C. Hanna, J.M. Olson, *Phys. Rev. B* 68 (2003) 035310.
- [34] B. Fluegel, S. Smith, Y. Zhang, A. Mascarenhas, J.F. Geisz, J.M. Olson, *Phys. Rev. B* 65 (2002) 115320.
- [35] D.E. McCumber, M.D. Sturge, *J. Appl. Phys.* 34 (1963) 1682.
- [36] E.N. Economou, M.H. Cohen, *Phys. Rev. Lett.* 24 (1970) 218.